

Boost Distribution System Restoration with Emergency Communication Vehicles Considering Cyber-Physical Interdependence

Zhigang Ye, *Member, IEEE*, Chen Chen, *Senior Member, IEEE*, Ruihuan Liu, *Student Member, IEEE*, Kai Wu, *Senior Member, IEEE*, Zhaohong Bie, *Senior Member, IEEE*

Abstract—Enhancing restoration capabilities of distribution systems is one of the main strategies for resilient power systems to cope with extreme events. However, most of the existing studies assume the communication infrastructures are intact for distribution automation, which is unrealistic. Motivated by the applications of the emergency communication vehicles (ECVs) in quickly setting up wireless communication networks after disasters, in this paper, we propose an integrated distribution system restoration (DSR) framework and optimization models, which can coordinate the repair crews, the distribution system (physical sectors), and the emergency communication (cyber sectors) to pick up unserved customers as quickly as possible. Case studies validated the effectiveness of the proposed models and proved the benefit of considering ECVs and cyber-physical interdependencies in DSR.

Index Terms—cyber-physical interdependence, distribution system restoration, emergency communication vehicles.

NOMENCLATURE

Sets

$\mathcal{D}^C, \mathcal{D}^R$	Depots with emergency communication vehicles (ECVs) /repair crews (RCs).
$\mathcal{W}^C, \mathcal{W}^R$	Working sites (WSs) for ECVs/RCs, where \mathcal{W}^R include switches (\mathcal{SW}) and faulted lines (\mathcal{F}), i.e., $\mathcal{W}^R = \mathcal{SW} \cup \mathcal{F}$.
$\mathcal{W}_{(i,j)}^C$	Working sites that can cover the feeder terminal unit (FTU) $(i,j)'$.
\mathcal{N}^C	Communication nodes.
\mathcal{N}_w^C :	Communication nodes covered by the ECV at WS w .
\mathcal{SW}	Switches, including automatic switches (\mathcal{AS}) and manual switches (\mathcal{MS}), i.e., $\mathcal{SW} = \mathcal{AS} \cup \mathcal{MS}$.
\mathcal{C}^E	Electrical node cells.
\mathcal{L}_c	Loads in the node cell c .

Parameters

n^{CA}, n^{RA}	Dimension of the route table of communication agents (CAs)/repair agents (RAs).
T_0	Start time for ECVs and RCs departing from depots.
T^{MAX}	The scheduled time horizon.
T_{ij}^C, T_{ij}^R	Travel time for ECVs/RCs traveling from i to j .
T_j^{Cmin}	Minimum duration of stay for ECVs at working site j .
T_f^{RP}	Repair time for RCs to repair faulted component f .

$T_{(i,j)}^{MS}$	Operation time for RCs to manually operate switch (i,j) .
$T_{(i,j)}^{AS}$	Operation time of operating switch (i,j) remotely.
Variables	
x_{ij}^C, x_{ij}^R	Elements of the route table of CAs/RAs.
t_i^{Ca}, t_i^{Cd}	Arrival/departure time of CAs at/from WS i .
t_i^R	Arrival time of RAs at WS i .
f_i^R	Repair completion time of node cell i .
t_i^E	The time when node cell i is energized
d_{ij}^{AO}, d_{ij}^{MO}	Binaries indicating if the switch (i,j) is automatically/ manually operated from end i to j .
$d_{ij}^{MO_e}, d_{ij}^{MO_{de}}$	Binaries indicating if the switch (i,j) is manually operated with/without electricity from end i to j .

I. INTRODUCTION

LARGE scale power outages caused by extreme events, such as natural disasters, cascading failures, and cyber-attacks, are becoming more and more frequent throughout the world, which reflects the deficiency of power systems to cope with extreme events of high impact low possibility (HILP) [1-3]. Thus, the ways to improve the resilience, including preparedness, resistance, responsiveness, and rapid restoration capabilities of the power systems, have been causing more and more attention. Compared to the transmission systems, the distribution systems are more vulnerable to disasters and closer to customers, which leads to that most of the power outages occurring in the distribution systems [4]. Hence, enhancing the restoration capability of distribution systems is a key direction to improve the resilience of power systems.

With the development of smart grid technology, the effective and efficient integration and interaction of power network infrastructure (physical systems) and information sensing, processing, intelligence, and control (cyber systems) feature modern distribution systems [5]. The increased situational awareness with smart meters and phasor measurement units (PMUs), and the advanced control capabilities such as automated feeder switching, have begun to increase the resilience of distribution systems through more effective and timely fault detection, isolation, and restoration (FDIR) [3].

Distribution system restoration (DSR) aims to restore the

Z. Ye is with the State Grid Jiangsu Electric Power Co Ltd, Nanjing, China, the School of Electrical Engineering, Xi'an Jiaotong University, Xi'an, China, and the School of Electrical Engineering, Southeast University, Nanjing, China (e-mail: yzhggoodluck@hotmail.com); C. Chen, R. Liu, Z. Bie, and K. Wu are

with the School of Electrical Engineering, Xi'an Jiaotong University, China (e-mails: morningchen@xjtu.edu.cn, rhliu@stu.xjtu.edu.cn, zhbie@mail.xjtu.edu.cn, wukai@mail.xjtu.edu.cn);

power service through an energization path from power sources to unserved customers [4]. Normally, the cyber sectors of distribution automation (DA) are intact for distribution system so that the quick DSR can be achieved through network topology reconfiguration by remotely monitoring and controlling the automatic feeder switches via feeder terminal units (FTUs). However, in the case of extreme events such as natural disasters, both the cyber and physical sectors of the integrated cyber-physical distribution power systems (CPDS) could be disrupted [6, 7]. In this case, the quick-service restoration through reconfiguration may not be achieved because: 1) the disrupted communication network disables the self-healing capabilities of DA; 2) an energization path may not exist because multiple physical damages may block all the possible energization paths. Thus, to pick up the unserved customers, the repair crews should go to the damaged components or switches to repair/operate them manually. In recent years, there have been extensive studies on the co-optimization and coordination of DSR and crew dispatch after large-scale power outages, represented by Arif [8], Chen [9], Lei [10], et al. However, all of these work assume the cyber sectors of the CPDS are intact so that the automatic switches can be controlled remotely, which is too ideal to be applied in the real-world DSR.

The wireless communication network has been widely adopted in the existing distribution automation (DA) system to support the communication and control between control center and controllable devices (such as remotely controlled switches) via FTUs. After an extreme event, the wireless communication infrastructure, e.g., base stations, may be disrupted. In such cases, the self-healing capability of DA will be ineffective due to disconnected communication links between FTUs and the control center, causing the switches failing to be controlled remotely. This may further prolong the restoration process of the power grid so that the intact FTUs, which are originally powered by the grid to be restored, will deplete their backup batteries. On the contrary, if we can restore the communication networks before depletion of the backup batteries for FTUs, the functionality of DA could be enabled for service restoration.

The emergency communication services, such as the wireless communication network setup by emergency communication vehicles (ECVs) or unmanned aerial vehicles (UAVs), have been successfully utilized after natural disasters at certain areas where communication restoration is urgent and repairing communication infrastructures takes substantial time and efforts [11]. Similarly, the emergency communication techniques with ECVs have the potential to enhance the DSR by achieving self-healing communications for DA. However, how to utilize emergency communication in coordination with the service restoration and crew dispatch decision has not been well considered in the literature.

Hence, motivated by the abovementioned challenges, in this paper, we formulate the interdependencies and cooperation models of emergency communication set-up with ECVs and distribution system restoration. We aim to find extensive ways to enhance the resilience of power systems under effective and efficient integration and interaction of cyber-physical power

systems.

The main contribution of this paper can be summarized as below:

1) We propose an integrated framework in which setting up emergency communication networks by ECVs, dispatching the repair crews, and operating switches in the distribution systems are coordinated to enhance the restoration capabilities of the distribution systems.

2) We formulate the ECVs' characteristics with a communication agent (CA) model, including the wireless communication cover range and mobility models.

3) We formulate the coordination of ECVs, repair crews, and switches with the interdependent constraints of CAs, repair agents (RAs), and electric agents (EAs).

The rest of this paper is organized as follows. Section II introduces the integrated DSR framework, followed by the detailed formulations described in Section III. In Section IV, we give the solution methodology. Then, we test the proposed models by case studies and discuss the numerical results in Section V. In the end, we conclude this paper in Section VI.

II. INTEGRATED FRAMEWORK

In this section, we propose an integrated distribution system restoration, considering the emergency communication set up by ECVs where the existing communication infrastructure is ineffective, as depicted in Fig. 1. The control center sends commands of dispatching repair crews and ECVs and operating automatic switches remotely. The repair crew can repair damaged components and operate both automatic and manual switches. The bidirectional communication links between automatic feeder switches and the control center are built through the emergency wireless communication network set up by ECVs and FTUs. The seamless coordination of three sectors, i.e., the repair crews, the distribution system (physical sectors), and emergency communication (cyber sectors) are considered to help restore the unserved customers as quickly as possible. In the next section, we introduce the optimization models of these sectors and their interdependencies.

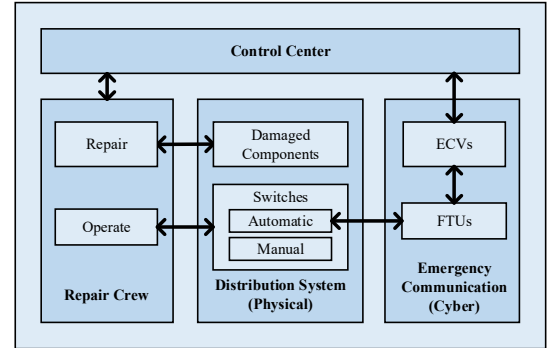


Fig. 1. Integrated distribution system restoration framework

III. PROBLEM FORMULATIONS

In this section, we formulate and explain the proposed optimization models step by step.

A. Emergency Communication Vehicle Model

An emergency communication vehicle (ECV) is actually a

mobile base station. When it is dispatched to and set up at a certain working site (WS), an ECV and the available communication nodes (CNs) within its cover range can form a wireless network. The working sites are certain locations given by expertized operators before dispatching the ECVs, in which many factors should be considered such as environment suitability for the erection of mobile base station, traffic accessibility for the vehicles, etc.

For a better explanation of the proposed ECV model, we use Fig. 2 to display the working process of ECVs. An ECV (e.g., v_1, v_2) departs from the depot where it is prepositioned. Then, it travels to a WS (e.g., v_1 to k_1 , v_2 to k_2), and sets up a temporary base station. Immediately, the ECV itself and the available CNs inside its cover range can quickly form a wireless network. The ECVs can also transfer bidirectional signals between the control center and the communication nodes which are coupled with physical devices. For example, the ECVs send status information received from feeder terminal units (FTUs)/remote terminal units (RTUs) to the control center and control commands to FTUs/RTUs from the control center.

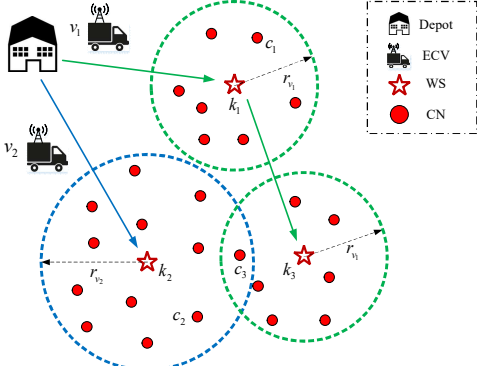


Fig. 2. Work process of emergency communication vehicles

An ECV can cover several CNs, and how many CNs can be covered is decided by its cover range. The cover range of an ECV v is modeled by a circle denoted by its radius r_v . We use a binary parameter $u_{v,k,c}$ to represent if a communication node c can be covered by the wireless network set up by ECV v at the working site k , and it can be calculated given the original data, as expressed below:

$$u_{v,k,c} = \varepsilon \left(r_v - \sqrt{(x_c - x_k)^2 + (y_c - y_k)^2} \right)$$

Where the step function: $\varepsilon(t) = \begin{cases} 1, & t \geq 0 \\ 0, & t < 0 \end{cases}$. For example, the CN c_1 is in the cover range of the base station set up by ECV v_1 at WS k_1 , so the parameter $u_{v_1,k_1,c_1} = 1$. Similarly, the parameter $u_{v_1,k_1,c_1} = 0$, $u_{v_2,k_2,c_2} = 1$. It should be noted that a CN can be covered by different ECVs at different WSs, which are determined by their relative locations. For example, the CN c_3 can be both covered by ECV v_1 at WS k_3 and by ECV v_2 at WS k_2 . Since the locations of CNs and WSs, as well as the cover range capability of ECVs (i.e., r_v) are known, the $u_{v,k,c}$ are given parameters for the dispatch of ECVs.

An ECVs can travel from one WS to another, setting up a wireless network to make some other intelligent physical devices observable and controllable. For example, in Fig. 2 ECV v_1 travels from WS k_1 to k_2 . The mobility of an ECV

essentially a “vehicle routing” problem, which has been widely studied in operational research areas. Differently, for ECVs, the duration of stay at WSs is a variable, not a parameter. To make it compatible with the models of repair crew and physical operational constraints of distribution systems, we adopt the “variable time step” (VTS) modeling method [9] to formulate the mobility of ECVs, and we add an extra variable t_i^{cd} (i.e., the departure time from WS i) so that the variable duration of stay can be modeled. Similar to [9], we use the concept of “communication agents” (CAs) to represent ECVs, and the specific constraints are formulated as below.

$$x_{ii}^c = 1, \forall i \in \mathcal{D}^c. \quad (1)$$

$$x_{ii}^c = 0, \forall i \in \mathcal{W}^c. \quad (2)$$

$$x_{ij}^c = 0, \forall i \in \mathcal{D}^c \cup \mathcal{W}^c, j \in \mathcal{D}^c, i \neq j. \quad (3)$$

$$x_{ij}^c + x_{ji}^c \leq 1, \forall i, j \in \mathcal{D}^c \cup \mathcal{W}^c. \quad (4)$$

$$\sum_{j=1, j \neq i}^n x_{ij}^c \leq n_{cap,i}^c, \forall i \in \mathcal{D}^c. \quad (5)$$

$$\sum_{j=1}^n x_{ij}^c \leq \sum_{h=1}^n x_{hi}^c \leq 1, \forall i \in \mathcal{W}^c. \quad (6)$$

$$t_i^{ca} = T_0, \forall i \in \mathcal{D}^c. \quad (7)$$

$$t_i^{ca} \leq t_i^{cd} \leq T^{MAX}, \forall i \in \mathcal{D}^c \cup \mathcal{W}^c. \quad (8)$$

$$t_j^{ca} \geq t_i^{cd} + T_{ij}^c - (1 - x_{ij}^c)M, \forall i \in \mathcal{D}^c \cup \mathcal{W}^c, j \in \mathcal{W}^c. \quad (9)$$

$$t_j^{ca} \leq t_i^{cd} + T_{ij}^c + (1 - x_{ij}^c)M, \forall i \in \mathcal{D}^c \cup \mathcal{W}^c, j \in \mathcal{W}^c. \quad (10)$$

$$t_j^{cd} \geq t_j^{ca} + T_j^{min} - (1 - \sum_{i=1, i \neq j}^n x_{ij}^c)M, \forall j \in \mathcal{W}^c. \quad (11)$$

$$t_j^{ca} \geq T^{MAX} - M \sum_{i=1, i \neq j}^n x_{ij}^c, \forall j \in \mathcal{W}^c. \quad (12)$$

$$t_j^{ca} \leq T^{MAX} + M \sum_{i=1, i \neq j}^n x_{ij}^c, \forall j \in \mathcal{W}^c. \quad (13)$$

Constraint (1–6) define the route table of communication agents (CAs). Specifically, (1–3) mean that a CA should travel starting only from depots and should not go back to depots. Constraint (4) represents that each possible route can be visited no more than once. Constraint (5) limits the total number of agents dispatched out of depot not to exceed the capacity of that depot. Besides, (6) depicts that each WS can be visited by at most one CA, and one CA should leave or stay at the visited WS. Except for route table-related constraints, (7–11) list the time-related constraints. Specifically, (7) defines the initial time of a CA in the time horizon. Constraint (8) ensures that, at any site (depot or WS), the departure time should be later than the arrival time, and both times not exceed the scheduled time horizon. Constraint (9) is tight only if there is a CA travels from i to j (i.e., the route table element $x_{ij}^c = 1$), which limits the time difference between arriving at site j and departing from the site i to exactly be the travel time from i to j . Constraint (10) ensures the duration of stay at a WS j should be longer than the required minimum duration if one CA is visiting this site. Constraint (11) sets the arrival time of a WS to be the end time of the scheduled horizon (i.e., T^{MAX}) if there are no CAs travel to that WS.

B. Crew Dispatch Model

To reduce the complexity of the crew dispatch model, first, we pre-assign working sites (WSs) of repair crews (including switches and faulted lines to be repaired) to depots. Similar to [12], the clustering model is formulated as follow:

$$\min \sum_{i \in \mathcal{D}^R} \sum_{j \in \mathcal{W}^R} y_{ij} T_{ij}^R \quad (p1)$$

$$\text{s.t. } \sum_{i \in \mathcal{D}^R} y_{ij} = 1, \forall j \in \mathcal{W}^R \quad (p2)$$

By solving the above integer programming problem, the optimal clustering strategy with minimum travel time can be

found. Then, we use the “repair agent” (RA) to represent repair crew, which can be modeled by variables of route table and arrival time list [9], which are listed below.

$$x_{ii}^R = 1, \forall i \in \mathcal{D}^R \quad (12)$$

$$x_{ii}^R = 0, \forall i \in \mathcal{W}^R \quad (13)$$

$$x_{ij}^R = 0, \forall i, j \in \mathcal{D}^R, i \neq j \quad (14)$$

$$x_{ij}^R + x_{ji}^R \leq 1, \forall i, j \in \mathcal{D}^R \cup \mathcal{W}^R \quad (15)$$

$$\sum_{j=1, j \neq i}^n x_{ij}^R \leq n_{cap,i}^R, \forall i \in \mathcal{D}^R \quad (16)$$

$$\sum_{j=1}^n x_{ij}^R \leq \sum_{h=1}^n x_{hi}^R \leq 1, \forall i \in \mathcal{W}^R \quad (17)$$

$$t_i^R = T_0, \forall i \in \mathcal{D}^R. \quad (18)$$

$$t_j^R \geq t_i^R + T_{ij}^R - (1 - x_{ij}^R)M \quad (19)$$

$$t_j^R \leq t_i^R + T_{ij}^R + (1 - x_{ij}^R)M \quad (19)$$

$$t_j^R \geq t_i^R + T_i^{RP} + T_{ij}^R - (1 - x_{ij}^R)M \quad (20)$$

$$t_j^R \leq t_i^R + T_i^{RP} + T_{ij}^R + (1 - x_{ij}^R)M \quad (20)$$

$$\forall i \in \mathcal{F} \setminus \mathcal{SW}, \forall j \in \mathcal{W}^R, i \neq j. \quad (20)$$

$$t_j^R \geq t_i^R + T_i^{MS} + T_{ij}^R - (1 - x_{ij}^R)M \quad (21)$$

$$t_j^R \leq t_i^R + T_i^{MS} + T_{ij}^R + (1 - x_{ij}^R)M \quad (21)$$

$$\forall i \in \mathcal{SW} \setminus \mathcal{F}, \forall j \in \mathcal{W}^R, i \neq j. \quad (21)$$

$$t_j^R \geq t_i^R + T_i^{RP} + T_i^{MS} + T_{ij}^R - (1 - x_{ij}^R)M \quad (22)$$

$$t_j^R \leq t_i^R + T_i^{RP} + T_i^{MS} + T_{ij}^R + (1 - x_{ij}^R)M \quad (22)$$

$$\forall i \in \mathcal{SW} \cap \mathcal{F}, \forall j \in \mathcal{W}^R, i \neq j. \quad (22)$$

$$t_j^R \geq T^{MAX} - M \sum_{i=1, i \neq j}^n x_{ij}^R \quad (23)$$

$$t_j^R \leq T^{MAX} + M \sum_{i=1, i \neq j}^n x_{ij}^R \quad (23)$$

$$f_{r^e(f)}^R \geq t_f^R + T_f^{RP}, \forall f \in \mathcal{F}. \quad (24)$$

$$f_i^R = T_0, \forall i \in \mathcal{C}^E, i \neq r^e(f), f \in \mathcal{F}. \quad (25)$$

In this paper, we assume all the crews have both skills of operating switches and repairing faulted lines, thus the operation agent (OA) and repair agent (RA) in [9] are unified to only be RA here. First, the form of the route table related constraints of RAs here in this paper (i.e., the constraints (12)–(17)) is the same as that of [9], but with a wider set of working sites (i.e., $\mathcal{W}^R = \mathcal{SW} \cup \mathcal{F}$). Please refer to [9] to see the detailed descriptions of these constraints. Second, the time-related constraints of RAs are listed in (18)–(25). Specifically, (18) defines the initial time of RAs in the scheduled time horizon. Constraints (19)–(22) describe the equality of arrival time between two sites if a RA can travel from one site to another. These constraints include: from a depot to a WS (i.e., (19)), from a faulted line (not switch) to another WS (i.e., (20)), from a healthy switch to another WS (i.e., (21)), and from a faulted switch to another WS (i.e., (22)). Constraint (23) sets the arrival time of a WS to be the end time of the scheduled horizon (i.e., T^{MAX}) if there are no RAs travel to that WS. Constraint (24)–(25) limit the repair completion time of different types of node cells, where $r^e(f)$ is the index transfer from RA to EA, which represents the node cell in which the fault f is inside. For a node cell with faulted lines inside of it, the repair completion time of this cell is larger than that of all the faulted lines inside it, as shown in (24). By contrast, for the node cell without faulted lines inside it, the repair completion time is set to be the initial time of RAs in the scheduled horizon, as shown in (25).

C. Physical System Model

We use the variable time step (VTS) modeling method, as

introduced in [4], to formulate the physical distribution systems. The virtual electric agents (EA) are used to represent the energy flow in the physical network, which departs from a substation or black-start DG and goes through node cells to restore unserved load in these cells. Specifically, the physical system models include 1) the constraints of EAs’ route table; 2) the constraints of EAs’ arrival time; 3) the constraints of energization status; 4) the constraints of system and component operation. All these constraints can be found in [4], and we integrate them labeled by one number, as summarized below.

TABLE I. THE INTEGRATED PHYSICAL SYSTEM MODEL

Number in this paper	Number in [4]	Description
	(1)–(6)	Constraints of the route table of EAs
	(7)–(9)	Constraints of the arrival time of EAs
	(12)–(22)	Constraints of the nodes’, cells’, and components’ energization status and their relationship
(E26)	(23)–(31), (37)–(42)	Constraints of the system operation (three-phase voltage and power equations), and the components’ operation (DGs, regulators, lines, and loads)

D. Interdependent Constraints

In the abovementioned models in section III.A–C, we use CAs, RAs, and EAs to represent the emergency communication vehicles, the repair crews, and the physical distribution systems, respectively. In this section, we list all the interdependent constraints among these agents.

1) CA-EA (Cyber-Physical) Interdependent Constraints

For healthy automatic switches, they can either be closed remotely or manually, which can be expressed as:

$$x_{ij}^E = d_{ij}^{AO} + d_{ij}^{MO}, \forall (i, j) \in \mathcal{AS} \setminus \mathcal{F}. \quad (27)$$

Basically, two conditions should be satisfied to enable the feeder automation to remotely close the opened switches: 1) the communication channel between the control center and the FTUs is set up to keep information flows smoothly; 2) the FTUs have power sources to keep their work. In this paper, we assume that in the short period (i.e., the scheduled time horizon), the existing communication infrastructure is not available and that the emergency wireless communication network can be set up by dispatching ECVs to certain working sites. According to the introduction in section III.A, when an ECV is dispatched to and set up at a WS, all the healthy FTUs inside the cover range can be involved in the wireless network and transfer information between the control center and FTUs installed at field automatic switches. On the other hand, the backup batteries of FTUs have limited capacity, so the residual time of FTUs (denoted as $RT_{(i,j)'}^E$) should also be considered. We formulate the cyber-physical interdependency between CA and EA as below.

$$d_{ij}^{AO} \leq \sum_{k \in \mathcal{W}_{(i,j)}^C} \sum_{h=1, h \neq k}^{n^{CA}} x_{hk}^C. \quad (28)$$

$$t_j^E \geq t_k^{Ca} - (2 - d_{ij}^{AO} - \sum_{h=1, h \neq k}^{n^{CA}} x_{hk}^C)M, \forall k \in \mathcal{W}_{(i,j)}^C. \quad (29)$$

$$t_j^E \leq t_k^{Cd} + (2 - d_{ij}^{AO} - \sum_{h=1, h \neq k}^{n^{CA}} x_{hk}^C)M, \forall k \in \mathcal{W}_{(i,j)}^C. \quad (30)$$

$$t_j^E \geq \max(t_i^E, f_i^R) + T_{(i,j)}^{AS} - (1 - d_{ij}^{AO})M. \quad (31)$$

$$RT_{(i,j)'}^E \geq \max(t_j^E, f_i^R) + T_{(i,j)}^{AS} - (1 - d_{ji}^{AO})M. \quad (32)$$

Constraints (28)–(32) gives the conditions that a healthy automatic switch $(i, j) \in \mathcal{AS} \setminus \mathcal{F}$ can be operated remotely,

where $(i, j)'$ is the FTU at the switch (i, j) , embedded with communication and control devices. Constraint (28) means if there are no ECVs traveling to the WSs that can cover the communication node of the FTU $(i, j)'$, then the automatic switch (i, j) cannot be closed remotely. Constraints (29)–(30) ensure that if the node cell j begin to be energized by remotely closing the automatic switch (i, j) from i to j (i.e., $d_{ij}^{AO} = 1$) and the FTU $(i, j)'$ is in the cover range of the ECV at WS k (i.e., $\sum_{h=1, h \neq k}^{n^{CA}} x_{hk}^c = 1$), then the energization time of node cell j should be during the stay of the ECV at WS k (i.e., $t_k^{CA} \sim t_k^{CD}$). In (31–32), the maximum of two time-related variables represents the “ready time” to switch on an automatic switch. For example, $\max(t_i^E, f_j^R)$ represent the ready time for the automatic switch (i, j) to be switched on from node cell i to j , which satisfies two conditions, i.e., 1) the node cell i has been energized, and 2) all the faults in the node cell j have been repaired. Similarly, $\max(t_j^E, f_i^R)$ represent the “ready time” of the automatic switch (i, j) to be switched on from node cell j to i . After outages caused by extreme events, the power supply of an FTU from the power grid is lost, and the backup battery of the FTU continues to supply it. It should also be noted that the power supply of FTU $(i, j)'$ from the power grid is only at one side of the switch (i, j) , normally the “from” node cell i . Thus, during the step-by-step restoration process, the “ready time” related constraints differ between the energization path “from i to j ” and “from j to i ” because of different power sources of FTU $(i, j)'$, as shown in (30–31). Specifically, (31) ensures that the switching on time of the node cell to be energized must be after the ready time, in which the “from” node cell has been restored and supply power for the FTU. On the contrary, if the automatic switch (i, j) is remotely switched on from the “to” node cell j to “from” cell i , the power supply of FTU $(i, j)'$ from the power grid is not applicable, and in this case, the switching on the process must be completed before the residual time of the backup battery of the FTU $(i, j)'$, as shown in (32).

2) RA-EA Interdependent Constraints

Any switch ($\forall (i, j) \in \mathcal{SW}$) can be closed manually, and the following constraints list the interdependent constraints between RA and EA when it is manually operated. Note that, in this paper, we assume all the repair crews are able to operate energized or de-energized switches.

$$d_{ij}^{MO} + d_{ji}^{MO} = \sum_{h=1, h \neq k}^{n^{RA}} x_{hk}^R, \forall (i, j) \in \mathcal{SW}, k = e^r(i, j). \quad (33)$$

$$d_{ij}^{MOe} + d_{ij}^{MOde} \geq 1 - (1 - d_{ij}^{MO})M, \forall (i, j) \in \mathcal{SW}. \quad (34)$$

$$d_{ij}^{MOe} + d_{ij}^{MOde} \leq 1 + (1 - d_{ij}^{MO})M, \forall (i, j) \in \mathcal{SW}. \quad (35)$$

$$\frac{t_{e^r(i,j)}^R - t_i^E}{M} \leq d_{ij}^{MOe} \leq \frac{t_{e^r(i,j)}^R - t_i^E}{M} + 1, \forall (i, j) \in \mathcal{SW}. \quad (35)$$

$$t_j^E \geq t_{e^r(i,j)}^R + T_{(i,j)}^{MS} - (2 - d_{ij}^{MO} - d_{ij}^{MOe})M, \forall (i, j) \in \mathcal{SW} \setminus \mathcal{F}. \quad (36)$$

$$t_j^E \geq t_{e^r(i,j)}^R + T_{(i,j)}^{RP} + T_{(i,j)}^{MS} - (2 - d_{ij}^{MO} - d_{ij}^{MOe})M, \forall (i, j) \in \mathcal{SW} \cap \mathcal{F}. \quad (37)$$

$$\frac{t_i^E - (t_{e^r(i,j)}^R + T_{(i,j)}^{MS})}{M} \leq d_{ij}^{MOde} \leq \frac{t_i^E - (t_{e^r(i,j)}^R + T_{(i,j)}^{MS})}{M} + 1, \forall (i, j) \in \mathcal{SW} \setminus \mathcal{F}. \quad (38)$$

$$\frac{t_i^E - (t_{e^r(i,j)}^R + T_{(i,j)}^{RP} + T_{(i,j)}^{MS})}{M} \leq d_{ij}^{MOde} \leq \frac{t_i^E - (t_{e^r(i,j)}^R + T_{(i,j)}^{RP} + T_{(i,j)}^{MS})}{M} + 1, \forall (i, j) \in \mathcal{SW} \cap \mathcal{F}. \quad (39)$$

$$\left. \begin{aligned} t_j^E &\geq t_i^E - (2 - d_{ij}^{MO} - d_{ij}^{MOde})M \\ t_j^E &\leq t_i^E + (2 - d_{ij}^{MO} - d_{ij}^{MOde})M \end{aligned} \right\}, \forall (i, j) \in \mathcal{SW}. \quad (40)$$

In these constraints, $e^r(i, j)$ denotes the index transfer from EA to RA, which represents the working site of the repair crews to repair and operate the switch (i, j) . Constraint (33–34) implies that if the switch (i, j) is visited by a RA, then it must be manually closed either from i to j or from j to i , and be either energized or de-energized during the operation. The constraints of energized and de-energized operation of the switch (i, j) are expressed in (35–37) and (38–40), respectively. For the energized operation of the switch (i, j) from i to j to energize the node cell j , the node cell i has been restored before a RA arrives at it, as shown in (35). In this case, the other node cell j will be restored immediately after the RA switching on (i, j) if (i, j) is healthy, or after the RA repairing and switching on (i, j) if (i, j) need to be repaired, as shown in (36–37). For the de-energized operation of the switch (i, j) from i to j , the node cell i can only be energized after the switch (i, j) has been repaired and closed, as shown in (38–39). In this case, both the node cell i and j will be restored immediately at the same time, as depicted in (40).

Except for manual operation constraints, we have additional RA-EA interdependent constraints are listed below.

$$t_i^E \geq t_{e^r(i,j)}^R + T_{(i,j)}^{RP}, \forall (i, j) \in \mathcal{SW} \cap \mathcal{F}. \quad (41)$$

$$t_j^E \geq t_{e^r(i,j)}^R + T_{(i,j)}^{RP}, \forall (i, j) \in \mathcal{SW} \cap \mathcal{F}. \quad (42)$$

Constraint (41) ensures both end cells of a faulted switch can only be energized after it is repaired. Constraint (42) limits the restoration time of any node cell must be after the repair completion time.

E. Objective Functions

We define the objective functions as below.

$$Obj^{EA} = \sum_{c \in \mathcal{CE}} \omega_c^{EA} t_c^{EA} \sum_{l \in \mathcal{L}_c} \sum_{\phi \in \Phi} P_{l,\phi}^L \quad (43)$$

$$Obj^{RA} = \omega_1^{RA} \sum_{i=1}^{n^{RA}} \sum_{j=1, j \neq i}^{n^{RA}} x_{ij}^R T_{ij}^R + \omega_2^{RA} \sum_{i=1}^{n^{RA}} f_i^R \quad (44)$$

$$\begin{aligned} Obj^{CA} = & \omega_1^{CA} \sum_{i=1}^{n^{CA}} \sum_{j=1, j \neq i}^{n^{CA}} x_{ij}^C T_{ij}^C + \\ & \omega_2^{CA} \sum_{i \in \mathcal{W}} (t_i^{CD} - t_i^{CA}) \end{aligned} \quad (45)$$

The proposed multi-objective functions include the EA, CA, and RA-related objectives, as depicted in (43–45) respectively. The Obj^{EA} in (43) is the EA related objective, which represents the total unserved energy of all the loads in cells with priorities (ω_c^{EA}). The Obj^{RA} in (44) is the RA related objective, which includes the total travel time of all the RAs and the total repair completion time of all the node cells, with different weights (ω_1^{RA} and ω_2^{RA}). The Obj^{CA} in (45) is the CA related objective, which also includes two parts, i.e., the total travel time of all the CAs and the total duration of stay of CAs at all the working sites, with different weights (ω_1^{CA} and ω_2^{CA}). In (43–45), all the coefficients (ω with superscript) are weights or priorities

inputted by the decision-makers.

F. The Whole Optimization Models

The integrated distribution system restoration optimization models are categorized into two types, according to whether the service restoration is with CAs (i.e., ECVs) or without CAs, which are respectively denoted as “OPT-WCA” and “OPT-WOCA”, i.e.:

OPT-WCA:

$$\text{Min. } Obj^+ = \beta^{EA} Obj^{EA} + \beta^{CA} Obj^{CA} + \beta^{RA} Obj^{RA} \quad (46)$$

s.t. CA's constraints: (1–11)

RA's constraints: (12–25)

EA's constraints: (E26)

Interdependent constraints: (27–42)

OPT-WOCA:

$$\text{Min. } Obj^- = \beta^{EA} Obj^{EA} + \beta^{RA} Obj^{RA} \quad (47)$$

s.t. RA's constraints: (12–25)

EA's constraints: (E26)

Interdependent constraints: (33–42)

In (46) and (47), the coefficients (β with superscript) are weights of the multi-objective functions, which are given by the decision-makers. By solving these two optimization problems individually, we can see the benefit of the ECVs regarding distribution system restoration.

IV. SOLUTION METHODOLOGY

The proposed optimization models (i.e., “OPT-WCA” and “OPT-WOCA”) are mixed-integer programming (MIP) problems, of which all the objective functions and constraints are linear except for the nonlinear terms $\max(\cdot)$ in (31–32). By linearizing these nonlinear terms, the whole models are transferred into mixed-integer linear programming (MILP) problems which can be effectively solved by the off-the-shelf solvers such as Cplex and Gurobi.

The maximum value of two variables ($y = \max\{x_1, x_2\}$) can be linearized by introducing two binary variables (d_1, d_2) [13], and the equivalent MILP formulations are listed below:

$$L_i \leq x_i \leq U_i, \forall i = 1, 2$$

$$y \geq x_i, \forall i = 1, 2$$

$$y \leq x_i + (U_{\max} - L_i)(1 - d_i), \forall i = 1, 2$$

$$d_1 + d_2 = 1$$

where L_i and U_i are lower and upper bound of the variable x_i , and U_{\max} is the maximum value of all the upper bounds. In our problems, according to the definition the variables t_i^E and f_j^R must be within the scheduled time horizon ($[0, T^{\max}]$). Thus, we use an auxiliary variable y_{ij} to replace the nonlinear term (i.e., $\max\{t_i^E, f_j^R\}$) in (31–32) and introduce two binary variables d_{ij}^E and d_{ij}^R to formulate the equivalent MILP constraints, as listed below:

$$y_{ij} \geq t_i^E \quad (A.1)$$

$$y_{ij} \geq f_j^R \quad (A.2)$$

$$y_{ij} \leq t_i^E + T^{\max}(1 - d_{ij}^E) \quad (A.3)$$

$$y_{ij} \leq f_j^R + T^{\max}(1 - d_{ij}^R) \quad (A.4)$$

$$d_{ij}^E + d_{ij}^R = 1 \quad (A.5)$$

where $\forall i, j \in \mathcal{C}^E, (i, j) \in \mathcal{AS} \setminus \mathcal{F}$. By adding the auxiliary constraints (A.1–A.5) to “OPT-WCA”, the problems become

MILP models.

V. CASE STUDY

In this section, we test the proposed optimization models on IEEE 123 node test feeder, solved by Cplex 12.8 on a PC with Intel Core i7-7500U 2.90-GHz CPU, 16-GB RAM, and 64-bit operating system.

A. Case Design and Parameters

We use the 123 node test feeder, which is a medium-size unbalanced distribution system operating at 4.16 kV nominal voltage with 3385 kW three-phase unbalanced loads in total [14]. The one-line diagram of the test system located in a rectangular coordinate system is shown in Fig. 3, in which all the nodes and lines are marked in grey and all the switches are open, which means they are all de-energized at the beginning of the scheduled horizon. Also, we assume the substation is initially unavailable and can start to supply power at the 30th minute.

As shown in Fig. 3, we have allocated 4 repair crews at 2 depots (2 crews at each one) to be prepared to visit 20 candidate working sites, including 4 faulted lines and 16 switches. By solving the integer programming problem (p1–p2), the 4 faulted lines are clustered into 2 depots, in which (13, 34) and (47, 48) belong to depot D1, (76, 77) and (101, 102) belong to depot D2. For the switches, we assume all of them are automatic switches installed with FTUs (labeled with red solid dots on the top of the switches) which can be communicated and controlled remotely. Besides, we assume all the switches could be either closed remotely through feeder automation or closed manually by repair crews.

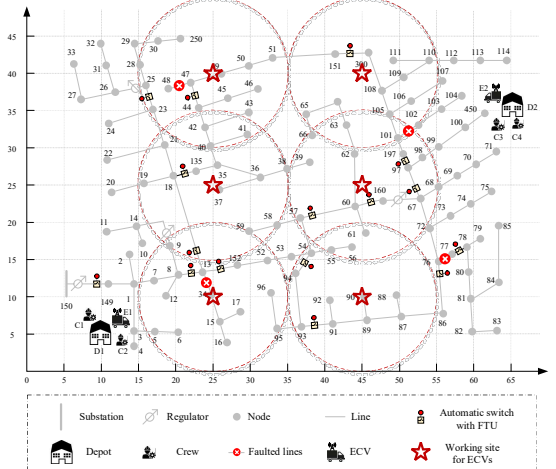


Fig. 3. The 123 node test feeder modified for case studies

As for the cyber part, we assume the existing communication network is unavailable, which means all the automatic switches are not able to be operated remotely if there is no emergency communication. In this section, we design two cases to validate the proposed models. In Case 1, we have 2 ECVs at the 2 depots (1 ECV at each one). The ECVs are prepared to visit 6 candidate working sites to set up an emergency wireless communication network, in which the cover ranges of these 2 ECVs are the same with a radius of 10 units, as labeled with dashed circles in Fig. 3. In Case 2, there are no ECVs available to be dispatched.

Case 1 and 2 are modeled by “OPT-WCA” and “OPT-WOCA” in Section III.F, respectively. By formulating and solving the two models, we can compare the optimal DSR schedules for these two cases. For the multi-objective functions in (43–47), we set: 1) $\omega_c^{EA} = 1$ for all the electric node cells; 2) $\omega_1^{RA} = \omega_2^{RA} = 1$ for repair agents; 3) $\omega_1^{CA} = \omega_2^{CA} = 1$ for communication agents; and 4) $\beta^{EA} = 10$, $\beta^{CA} = \beta^{RA} = 1$ for different agents.

For other parameters, we set: 1) the time horizon: 12 hours; 2) the repair time of faults lines: 2 hours for each one; 3) the travel time for repair crews and ECVs traveling between two sites: be proportional to the Euclid distances in Fig. 3, in which the maximum is 65 minutes between depot D1 and depot D2; 4) switching time for remote operation: 1 minute; 5) switching time for manual operation: 15 minutes; and 6) the residual time for FTUs: 4 hours for each one.

B. Results and Discussions

The two models are solved by Cplex 12.8 with 0.001 MIP Gap, and the optimal solutions for Case 1 and 2 are obtained with 93.51 and 4.67 seconds computation time, respectively.

For Case 1 and 2, the physical system is fully energized and all the loads (3385 kW) are restored after the 219th and 278th minutes, respectively. The multiple objective values (Obj^{EA} , Obj^{RA} and Obj^{CA}) and the total objective values (Obj^+ , Obj^-) for Case 1 and 2 are listed in Table II.

TABLE II. OBJECTIVE VALUES FOR CASE 1 AND 2

No.	Obj^{EA} (kWh)	Obj^{RA} (Min.)	Obj^{CA} (Min.)	Obj^+	Obj^-
Case 1	8651	1012	247	87772	-
Case 2	11363	1022	-	-	114900

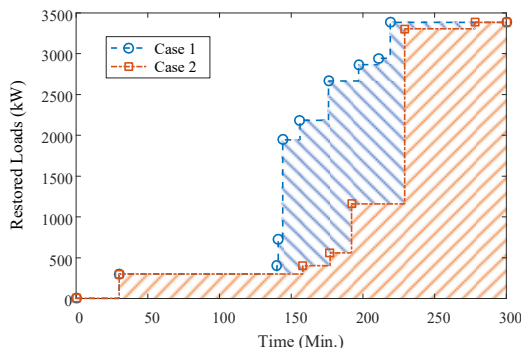


Fig. 4. Total restored loads (in kW) of Case 1 and 2

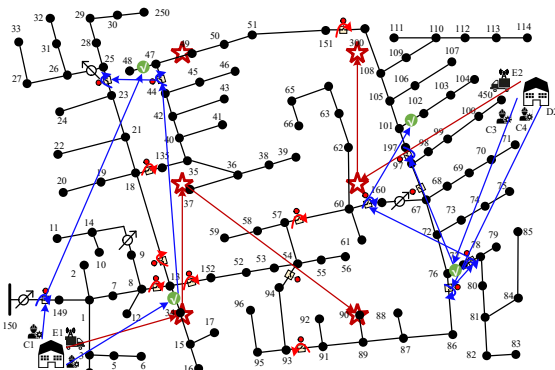


Fig. 5. RAs' and CAs' routes of Case 1

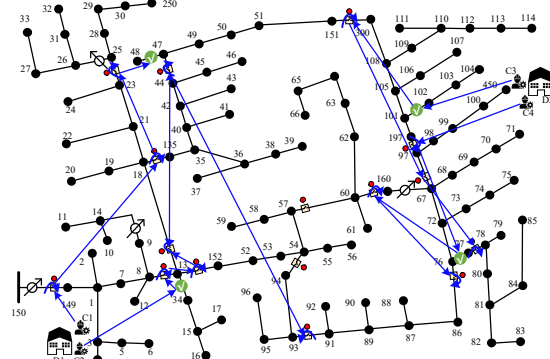


Fig. 6. RAs' routes of Case 2

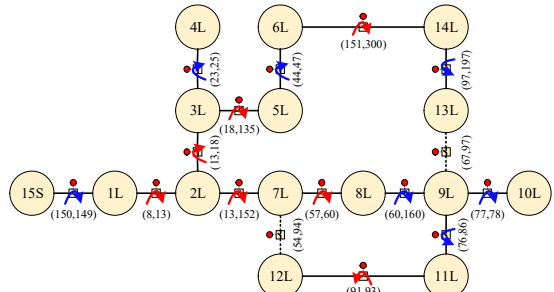


Fig. 7. The EA's route of Case 1.

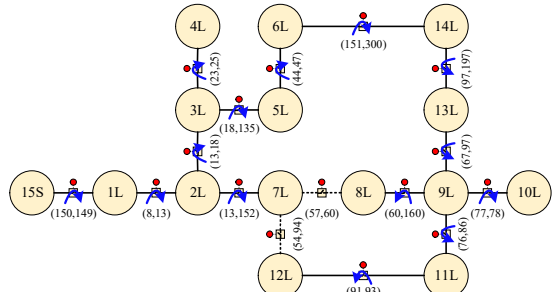


Fig. 8. The EA's route of Case 2.

Compared to Case 2, Case 1 (with ECVs or CAs) has less unserved energy (i.e., Obj^{EA}) at the cost of dispatching ECVs to set up wireless communication networks, which proves the benefit of leveraging ECVs to enhance the power system's restoration and resilience when the cyber sectors of the distribution automation (DA) system are damaged. As formulated in (44–45), the objective value of RA represents the total travel time and repair completion time, while the objective value of CA represents the total travel time and duration of stay, and both objective values reflect the time cost of dispatching emergency resources to help power recovery. The total objective values of Case 1 and 2 are mainly decided by Obj^{EA} , because the weights of Obj^{EA} , Obj^{RA} , and Obj^{CA} are 10, 1, and 1, which means restoring the unserved customers as quickly as possible has the highest priority compared with dispatching repair crews and ECVs. More specific DSR processes for both cases are displayed below, in which Fig. 4 compares the restored loads between Case 1 and 2; Fig. 5 presents the RAs' and CAs' routes of Case 1; Fig. 6 presents the RAs' routes of Case 2; Fig. 7–8 simplify the EA's routes of Case 1–2 with only node cells and switches left; and Table II lists the switching

sequences and energized node cells of both cases.

TABLE III SWITCHING SEQUENCE AND ENERGIZED NODE CELLS

Case 1			Case 2		
Time (Min.)	Op. (Switch)	ENCs	Time (Min.)	Op. (Switch)	ENCs
18	<i>MD</i> (150,149)	-	18	<i>MD</i> (150,149)	-
30	Substation	15S, 1L	30	Substation	15S, 1L
39	<i>MD</i> (76,86)	-	32	<i>MD</i> (97,197)	-
57	<i>MD</i> (77,78)	-	52	<i>MD</i> (18,135)	-
87	<i>MD</i> (60,160)	-	76	<i>MD</i> (23,25)	-
140	A (8,13)	2L	158	ME (8,13)	2L
141	A (13,18) A (13,152)	3L 7L	165	<i>MD</i> (151,300)	-
144	A (57, 60)	8L, 9L, 10L, 11L	177	ME (13,152)	7L
156	A (18,135)	5L	192	ME (13,18)	3L, 4L, 5L
173	<i>MD</i> (97,197)	-	195	<i>MD</i> (60,160)	-
176	ME (44,47)	6L	202	<i>MD</i> (67,97)	-
197	ME (23,25)	4L	224	<i>MD</i> (76,86)	-
211	A (91,93)	12L	226	<i>MD</i> (77,78)	-
219	A (151, 300)	14L, 13L	229	ME (44,47)	6L, 4L, 13L, 9L, 8L, 10L, 11L
			278	ME (91,93)	12L

Op.(Switch): operation mode for switches; *MD*: manual de-energized operation; *ME*: manual energized operation; *A*: automatic operation; ENCs: energized node cells; S: substation cell; L: load cell.

Fig. 4 shows that Case 1 restores more energy than Case 2, and the extra blue shaded area represents the difference of restored energy between Case 1 and 2, which can be explained by Fig. 5–8 and Table III. The crew repair faulted lines and operate switches sequentially by traveling among these working sites, represented by the RAs' routes, which are labeled with blue arrows in Fig. 5–6. The ECVs set up wireless communication networks sequentially by traveling among candidate working sites, represented by the CAs' routs, which are labeled with red arrows in Fig. 5. By comparing Fig. 5 and 6, it can be found that, in Case 1, there are 7 switches operated remotely but not manually by crews. This is because the switches can communicate with and be controlled by the control center by the FTUs through the emergency wireless network set up by ECVs. As operating switches remotely is generally much quicker than operating them manually (e.g., 1 minute versus 15 minutes in our cases), the overall effect is that the restoration completion time of Case 1 is earlier than that of Case 2.

More specific interdependencies during the DSR can be found in Fig. 7–8 and Table III. In Case 1, as labeled with red arrows in Fig. 7 and the letter “*A*” in Table III, the automatic operation of switches advances switching sequence and restoration time. The manual operation of switches, as labeled with blue arrows in Fig. 8, includes de-energized (“*MD*” in Table III) and energized (“*ME*” in Table III) operation, of which the former cannot energize node cells while the latter can. The

pick times, as labeled with bold font in Table III, are the times when there are node cells energized and loads picked up, which exactly corresponds to the time steps in Fig. 4.

By the above-mentioned analysis, we can conclude that setting up a wireless communication network by dispatching ECVs can enable the automatic switches to be controlled remotely, which reduces travel time and switching time by repair crews and speeds the restoration of power systems. The spatial movement of the ECVs in cyber sectors causes the benefits of temporal savings in the restoration of power or physical sectors.

VI. CONCLUSION

In this paper, we firstly propose an integrated distribution system restoration framework, which considers the cooperation and coordination of the repair crews, the distribution system (physical sectors), and emergency communication (cyber sectors). Then, we give the specific optimization models and solution methodology of the proposed models. Finally, the case studies validated the effectiveness and exhibited the benefit of considering ECVs and cyber-physical interdependencies in DSR.

VII. REFERENCES

- [1] Y. Wang, C. Chen, J. Wang, and R. Baldick, "Research on Resilience of Power Systems Under Natural Disasters—A Review," *IEEE Transactions on Power Systems*, vol. 31, no. 2, pp. 1604-1613, 2016.
- [2] Z. Li, M. Shahidehpour, F. Aminifar, A. Alabdulwahab, and Y. Al-Turki, "Networked Microgrids for Enhancing the Power System Resilience," *Proceedings of the IEEE*, vol. 105, no. 7, pp. 1289-1310, 2017.
- [3] U. S. DOE, "Economic Benefits of Increasing Electric Grid Resilience to Weather Outages," 2013, Available: https://www.energy.gov/sites/prod/files/2013/08/f2/Grid%20Resiliency%20Report_FINAL.pdf.
- [4] B. Chen, Z. Ye, C. Chen, and J. Wang, "Toward a MILP Modeling Framework for Distribution System Restoration," *IEEE Transactions on Power Systems*, vol. 34, no. 3, pp. 1749-1760, 2019.
- [5] X. Yu and Y. Xue, "Smart Grids: A Cyber-Physical Systems Perspective," *Proceedings of the IEEE*, vol. 104, no. 5, pp. 1058-1070, 2016.
- [6] A. Kwasinski, "Lessons from Field Damage Assessments about Communication Networks Power Supply and Infrastructure Performance during Natural Disasters with a focus on Hurricane Sandy," 2013, Available: <http://users.ece.utexas.edu/~kwasinski/1569715143%20Kwasinski%20paper%20FCC-NR2013%20submitted.pdf>.
- [7] J. Lu, X. Xie, X. Zhou, and C. Bu, "Research on power-communication coordination recovery strategy based on grid dividing after extreme disasters," *IOP Conference Series: Earth and Environmental Science*, vol. 675, 2021.
- [8] A. Arif, Z. Wang, J. Wang, and C. Chen, "Power Distribution System Outage Management With Co-Optimization of Repairs, Reconfiguration, and DG Dispatch," *IEEE Transactions on Smart Grid*, vol. 9, no. 5, pp. 4109-4118, 2018.
- [9] B. Chen, Z. Ye, C. Chen, J. Wang, T. Ding, and Z. Bie, "Toward a Synthetic Model for Distribution System Restoration and Crew Dispatch," *IEEE Transactions on Power Systems*, vol. 34, no. 3, pp. 2228-2239, 2019.
- [10] S. Lei, C. Chen, Y. Li, and Y. Hou, "Resilient Disaster Recovery Logistics of Distribution Systems: Co-Optimize Service Restoration With Repair Crew and Mobile Power Source Dispatch," *IEEE Transactions on Smart Grid*, vol. 10, no. 6, pp. 6187-6202, 2019.
- [11] V. Y. Kishorbhai and N. N. Vasantbhai, "AON: A Survey on Emergency Communication Systems during a Catastrophic Disaster," *Procedia Computer Science*, vol. 115, pp. 838-845, 2017/01/01/2017.
- [12] Z. Ye, C. Chen, B. Chen, and K. Wu, "Resilient Service Restoration for Unbalanced Distribution Systems With Distributed Energy Resources by Leveraging Mobile Generators," *IEEE Transactions on Industrial Informatics*, vol. 17, no. 2, pp. 1386-1396, 2021.
- [13] F. X. O. Suite. (2009). *MIP formulations and linearizations - Quick reference*. Available: <https://docplayer.net/53911163-Mip-formulations-and-linearizations-quick-reference.html>
- [14] C. IEEE PES Power System Analysis, and Economics Committee. (1992). *IEEE 123 Node Test Feeder*. Available: <https://site.ieee.org/pes-testfeeders/resources/>